Impact of RF Impairments on the Performance of Multi-carrier and Single-carrier based 60 GHz Transceivers

Umar H. Rizvi, Gerard J. M. Janssen, and Jos H. Weber
IRCTR/CWPC, Wireless and Mobile Communications Group,
Faculty of Electrical Engineering, Mathematics and Computer Science,
Delft University of Technology, Delft, The Netherlands.
Email(s): {u.h.rizvi, g.janssen, j.h.weber}@ewi.tudelft.nl

***Abstract*— The 60 GHz band, with a large unlicensed bandwidth, is an excellent choice for short distance high-speed communications. However, radio frequency (RF) circuit limitations at 60 GHz give rise to impairments such as phase noise, in-phase/quadrature-phase (I/Q) imbalance and amplifier nonlinearities. The candidate transmission schemes, in addition to multi-path fading, should therefore be fairly robust against RF circuit imperfections. This paper investigates the performance degradation as a function of various circuit parameters for multi-carrier (MC) and single-carrier (SC) schemes, which can be useful for: i) performing a system cost and performance trade-off comparison, ii) identifying main performance bottle necks for MC and SC based systems.**

I. Introduction

Multi-carrier (MC) and single-carrier (SC) schemes are two practical alternatives for high data rate communications in the 60 GHz band. While both schemes can counter inter-symbol-interference (ISI) at a reasonable implementation complexity [1], they have different tolerances to RF circuit imperfections. A number of comparisons between MC and SC schemes can be found in the literature [2], [3], [4]. The SC scheme is known to have a lower peak-to-average-power ratio (PAPR) and a higher resistance to frequency offset errors [2]. The SC scheme with block based processing can achieve maximum diversity in multi-path fading environments [2] and therefore performs better in un-coded scenarios. For code rates $R_c \leq 1/2$ and assuming an ideal front end, SC and MC schemes exhibit similar performance in IEEE 802.11 [2] and 60 GHz transmission scenarios [3]. The SC scheme was shown to require a lower input back-off (IBO) for the high power amplifier (HPA) and has a similar sensitivity to phase noise (PN) and in-phase/quadrature-phase (I/Q) imbalance for IEEE 802.11 transmission scenarios [4]. This however is not expected to be the case for 60 GHz transmission scenarios and is therefore investigated in detail.

In this paper, the impact of RF circuit imperfections on MC and SC schemes is investigated, based on RF circuit transfer characteristics that are in accordance with 60 GHz devices proposed in literature [5], [6]. The RF imperfections taken into account are: oscillator PN, I/Q imbalance and amplifier nonlinearities. The performance degradation in signal-to-noise ratio (SNR) is determined as a function of the bit error rate (BER) for various circuit parameters. It is shown that the SC scheme has a lower tolerance to phase noise, whereas it is more robust to amplifier nonlinearities and I/Q imbalance. The results presented in this paper helps the 60 GHz system designer to make various system choices. For example, they can be used to determine the required coding gain for SC and MC schemes when used in 60 GHz transmission scenarios.

II. System and Channel Model

This section presents a brief outline of orthogonal frequency division multiplexing (OFMD) based MC schemes [2], block based SC transmission schemes with frequency domain equalization (FDE) [1], their overall system complexity and a LOS 60 GHz transmission channel model. Both the SC and the MC schemes were shown to have the same implementation complexity [7].

Notation: Vectors are denoted by boldface letters. The time and frequency domain variables are represented by lower and upper case letters, respectively. Superscript † stands for complex conjugate. The $k-$th sample for an N point forward and inverse fast Fourier transform (FFT/IFFT) of a complex vector $\mathbf{v}$ is denoted by $\mathcal{F}_k(\mathbf{v})$ and $\mathcal{F}_k^{-1}(\mathbf{v})$, respectively. The boldface letter $\mathbf{h}$ denotes the channel impulse response (CIR) and $\mathbf{n}$ denotes a vector of complex white Gaussian noise samples with zero mean and variance $N_0/2$ per dimension. The elements of vector $\mathbf{n}$ are assumed to be independent and identically distributed (i.i.d). The linear and circular convolution operations are denoted by $*$ and $\otimes$, respectively.

A. 60 GHz Transmission Channel Model

A line-of-sight (LOS) time invariant tapped delay line (TDL) channel model, based on wideband measurements at 60 GHz [8], is used for performance evaluation. The channel coefficients h_n, given in [8], are modeled as complex numbers with a uniformly distributed phase between $[0, 2\pi)$. This channel has an average root mean square (RMS) delay spread of $\overline{\tau}_{rms} = 7$ ns and an average maximum delay spread of $\overline{\tau}_{max} = 70$ ns. The channel coherence bandwidth B_c can be given as $B_c = 0.063/\overline{\tau}_{rms} = 9$ MHz.

B. Multi-carrier based System Design

For an OFDM based MC system shown in Figure 1, the mapped data symbol vector $\mathbf{x} = (x_0, x_1, \ldots, x_{N-1})$,

1-4244-1370-2/07/$25.00 ©2007 IEEE

is passed though an IFFT block to produce an OFDM symbol $\mathbf{X} = \left(\mathcal{F}_0^{-1}(\mathbf{x}), \ldots, \mathcal{F}_{N-1}^{-1}(\mathbf{x})\right)$, where $\mathcal{F}_k^{-1}(\mathbf{x}) = \frac{1}{N}\sum_{n=0}^{N-1} x_n e^{j2\pi kn/N}$. The OFDM symbol length N is chosen such that the OFDM symbol time $T_N = N/B = NT_s$ is much larger than the channel delay spread. Here B denotes the system bandwidth and T_s denotes the system sampling time given by $T_s = 1/B$. Inter-block interference (IBI) between adjacent OFDM symbols is prevented by the addition of a cyclic prefix (CP). The CP, which consists of the last L samples of the OFDM block is chosen larger than the maximum channel delay spread i.e. $L \geq N_{max}$, where $N_{max} = \lceil \overline{\tau}_{max}/T_s \rceil$ gives the maximum average channel delay spread in samples. The OFDM symbol after CP insertion is given as $\mathbf{X}^C = (X_{N-L}, X_{N-L+1}, \ldots, X_{N-1}, X_0, X_1, \ldots, X_{N-1})$.

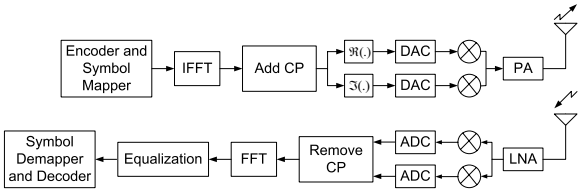

Fig. 1. A simplified system model for a MC based transceiver

Assuming an ideal front end, the received vector after passing through the channel is given as $\mathbf{Y}^C = \mathbf{X}^C * \mathbf{h} + \mathbf{n}^C$ where $\mathbf{n}^C$ is a vector of Gaussian noise samples with zero mean and variance $N_0/2$. The CP removal converts linear convolution into circular convolution $\mathbf{Y} = \mathbf{X} \otimes \mathbf{h} + \mathbf{n}$, where $\mathbf{Y}$ denotes the CP removed vector. After FFT, the samples of vector $\mathbf{y}$ are given as $y_m = x_m \mathcal{F}_m(\mathbf{h}) + \mathcal{F}_m(\mathbf{n})$ where $\mathcal{F}_m(\mathbf{h}) = \sum_{n=0}^{N-1} h_n e^{-j2\pi mn/N}$. Assuming perfect channel state information (CSI) at the receiver, a simple (but sub-optimum) equalization strategy is to perform a point wise division of the FFT output by the estimated channel transfer function i.e. $\hat{x}_m = y_m/\mathcal{F}_m(\mathbf{h}) = x_m + \frac{\mathcal{F}_m(\mathbf{n})}{\mathcal{F}_m(\mathbf{h})}$. The equalized symbol vector $\hat{\mathbf{x}}$ is then passed to a maximum likelihood (ML) detector that operates on a symbol by symbol basis. The parameters of the 60 GHz OFDM based transceiver under consideration in this paper are summarized in Table I. The performance of MC-QPSK and MC-8PSK schemes when used with an ideal front end is shown in Figure 2.

TABLE I
MC AND SC SYSTEM PARAMETERS

	MC	**SC**
Carrier frequency	60 GHz	60 GHz
Modulation scheme	QPSK / 8PSK	QPSK / 8PSK
Channel bandwidth	1 GHz	1 GHz
# of sub-carriers / block length	1024	1024
Sub-carrier spacing	976.56 KHz	-
Cyclic prefix length (L)	100	100

C. Single-carrier based System Design

The complexity limitation of the SC scheme has recently been overcome with the introduction of frequency domain

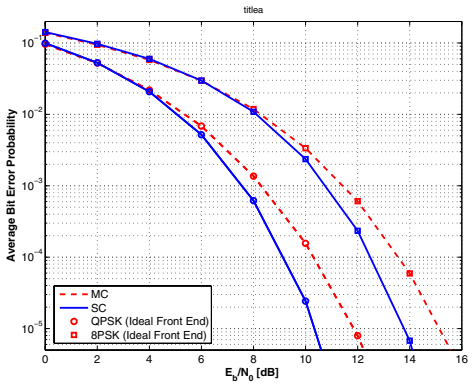

Fig. 2. Performance of MC and SC based transceivers at 60 GHz employing QPSK/8PSK constellations for an ideal front end

equalization (FDE) [1]. In a SC-FDE system shown in Figure 3, the mapped data symbol vector $\mathbf{x} = (x_0, x_1, \ldots, x_{N-1})$ is added with a CP of length L prior to transmission. The vector to be transmitted is thus given by $\mathbf{x}^C = (x_{N-L}, x_{N-L+1}, \ldots, x_{N-1}, x_0, x_1, \ldots, x_{N-1})$.

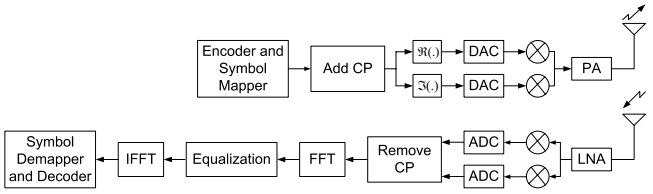

Fig. 3. A simplified system model for a SC based transceiver

Assuming an ideal front end, the received signal vector after passing through the channel is given by $\mathbf{r}^C = \mathbf{x}^C * \mathbf{h} + \mathbf{n}^C$. The received vector $\mathbf{r}$ after CP removal is given by $\mathbf{r} = \mathbf{x} \otimes \mathbf{h} + \mathbf{n}$. The samples of vector $\mathbf{Y}$, after FFT are given as $Y_m = \mathcal{F}_m(\mathbf{h})\mathcal{F}_m(\mathbf{x}) + \mathcal{F}_m(\mathbf{n})$. Assuming perfect CSI at the receiver, a simple (but sub-optimum) equalization strategy is to perform a point wise division of the FFT output by the estimated channel transfer function i.e. $\hat{Y}_m = Y_m/\mathcal{F}_m(\mathbf{h}) = \mathcal{F}_m(\mathbf{x}) + \frac{\mathcal{F}_m(\mathbf{n})}{\mathcal{F}_m(\mathbf{h})}$. The components of the vector $\hat{\mathbf{x}}$ after IFFT operation are given as $\hat{x}_m = x_m + \mathcal{F}_m^{-1}(\mathbf{N})$, where $\mathbf{N} = (\mathcal{F}_0(\mathbf{n})/\mathcal{F}_0(\mathbf{h}), \ldots, \mathcal{F}_{N-1}(\mathbf{n})/\mathcal{F}_{N-1}(\mathbf{h}))$. The estimated data symbol vector $\hat{\mathbf{x}}$ is then passed to an ML detector. The system parameters for the 60 GHz SC based system design under consideration in this paper are given in Table I. The performance of SC-QPSK and SC-8PSK schemes when used with an ideal front end is shown in Figure 2.

III. RF Impairments: Models and Consequences

This section compares the performance of SC and MC based transceivers in the presence of RF circuit imperfections. The front end impairments taken into account are: PN, amplifier nonlinearities and I/Q imbalance. The samples of the received symbol $\hat{\mathbf{x}}$, after CP removal and equalization in the presence of RF imperfections are given by

$$\hat{x}_m = \kappa_m x_m + \zeta_m + \eta_m, \quad (1)$$

where κ_m, ζ_m are impairment and transmission scheme dependent multiplicative and additive terms, η_m is due to additive white Gaussian noise (AWGN) and x_m is a sample from the original transmitted vector $\mathbf{x}$. The factors κ_m and ζ_m will be explained in subsequent sections. The vector $\hat{\mathbf{x}}$ is then passed to a maximum likelihood (ML) detector that works on a symbol by symbol basis. For MC transmissions, η_m is given by $\eta_m = \mathcal{F}_m(\mathbf{n})/\mathcal{F}_m(\mathbf{h})$ and for SC based systems $\eta_m = \mathcal{F}_m^{-1}(\mathbf{N})$.

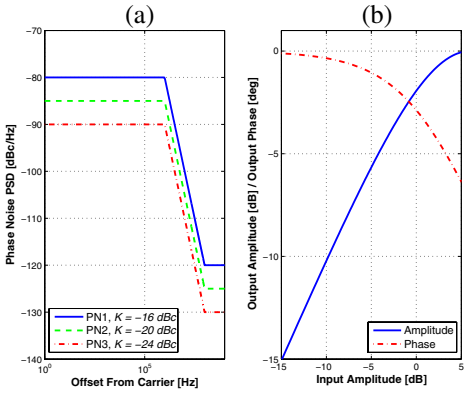

Fig. 4. Transfer characteristics for (a) PN and (b) Nonlinear HPA

A. Phase Noise: Model and Consequences

Non-ideal oscillators give rise to PN and in our system it is assumed that the phase is tracked with a 60 GHz phase locked loop (PLL). This gives rise to a particular power spectral density (PSD) (instead of a Dirac pulse at the carrier frequency). The PN PSD is usually characterized by 3 parameters [9] i.e. the total double sided integrated PSD K in dBc, the PN spectrum bandwidth f_o in Hz and the noise floor $\mathcal{L}$ in dBc/Hz. Three PN models each with $f_o = 1$ MHz, a $\mathcal{L}$ of -120 dBc/Hz (PN1), -125 dBc/Hz (PN2) and -130 dBc/Hz (PN3), and a K of -16 dBc, -20 dBc and -24 dBc, respectively, are considered. These models are shown in Figure 4. These models match quite well, the measured phase noise spectra of 60 GHz phase locked loops (PLLs) [6]. For each OFDM symbol or SC block phase noise samples are generated according to the PSD in Figure 4.

The received signal for a MC system in the presence of transmitter phase noise, after CP removal is given as $\mathbf{Y} = \tilde{\mathbf{X}} \otimes \mathbf{h} + \mathbf{n}$, where $\tilde{\mathbf{X}}$ represents the phase noise perturbed OFDM symbol vector whose samples are given by $\tilde{X}_k = X_k e^{j\theta_k}$ and θ_k represents phase noise. After FFT and channel equalization the received signal is given by $\hat{x}_m = \mathcal{F}_m\left(\tilde{\mathbf{X}}\right) + \frac{\mathcal{F}_m(\mathbf{n})}{\mathcal{F}_m(\mathbf{h})}$, where $\mathcal{F}_m\left(\tilde{\mathbf{X}}\right)$ can be written as $\mathcal{F}_m\left(\tilde{\mathbf{X}}\right) = \left((1/N)\sum_{k=0}^{N-1} e^{j\theta_k}\right) x_m + (1/N)\sum_{n=0,n\neq m}^{N-1}\sum_{k=0}^{N-1} x_n e^{j2\pi(n-m)k/N} e^{j\theta_k}$. The multiplicative and additive terms are thus given by $\kappa_m = (1/N)\sum_{k=0}^{N-1} e^{j\theta_k}$ and $\zeta_m = (1/N)\sum_{n=0,n\neq m}^{N-1}\sum_{k=0}^{N-1} x_n e^{j2\pi(n-m)k/N} e^{j\theta_k}$, respectively. From the above equations it can be seen that the multiplicative factor κ_m, is the same for all symbols and is referred to as the common phase rotation (CPR). The additive ζ_m is a consequence of the orthogonality loss in the sub-carriers due to θ_k and is known as the inter-carrier interference (ICI). This additive term is seen to be dependent on the number of sub-carriers N, the mapped symbols $\mathbf{x}$ and θ_k.

For a block based SC scheme with FDE, the received signal after channel equalization is given by $\hat{x}_m = x_m e^{j\theta_m} + \mathcal{F}_m^{-1}(\mathbf{N})$. The interference terms are thus given as $\kappa_m = e^{j\theta_m}$ and $\zeta_m = 0$, where θ_m denotes the phase noise. It can be seen from the above equations that for a SC system the PN θ_m is directly multiplied with the baseband modulated symbol x_m. This results in rotation of the symbol constellation points. Since no orthogonal sub-carriers are involved in SC transmission, there is no ICI and thus $\zeta_m = 0$.

The performance degradation in the MC scheme is due to the CPR κ_m and additive ICI ζ_m, whereas for the SC scheme PN is directly multiplied with the transmitted symbol resulting in constellation rotation. For high phase noise variances and/or closely spaced constellation points the constellation clustering due to ICI term in MC scheme can help to counter constellation rotation and thus give better performance as compared to the SC scheme. Figure 5 gives the SNR degradation Δ_{SNR} as a function of BER for SC and MC schemes using QPSK and 8PSK signal constellations. The MC-QPSK scheme outperforms SC-QPSK by about 5.5 dB at a BER of 10^{-4} for a high phase noise variance i.e. PN1. For 8PSK, the MC scheme outperforms the SC scheme even at low phase noise variances, for example at a low phase noise variance i.e. PN3, MC-8PSK performs 0.9 dB better than SC-8PSK at a BER of 10^{-4}.

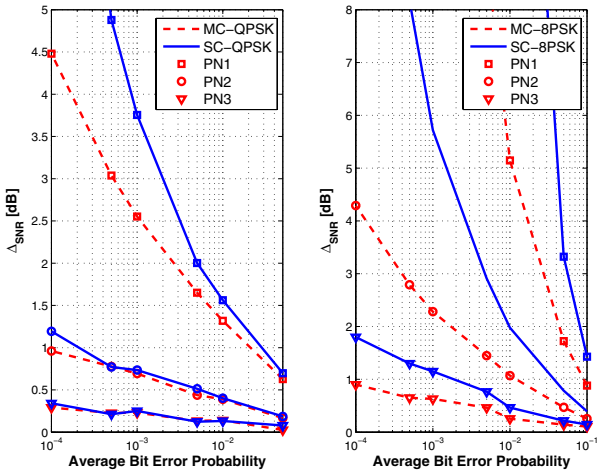

Fig. 5. SNR degradation as a function of BER for various PN models

B. I/Q Imbalance: Model and Consequences

A complex vector $\mathbf{a}$ in the presence of I/Q imbalance characterized by amplitude imbalance ϵ and phase imbalance ϕ is given by $\alpha\mathbf{a} + \beta\mathbf{a}^{\dagger}$, where $\alpha = \frac{1+\epsilon e^{-j\phi}}{2}$ and $\beta = \frac{1-\epsilon e^{j\phi}}{2}$ [10]. This implies that $\epsilon = 1, \phi = 0$ is the ideal situation. Two 60 GHz receiver architectures with an amplitude imbalance

of 1 dB and 1.6 dB and a phase error of 4° and 6.5° have been reported in [11]. We therefore use four I/Q models to investigate the impact of I/Q imbalance on SC and MC transceivers. These models are shown in Table II.

TABLE II

I/Q IMBALANCE PARAMETERS FOR 60 GHZ TRANSCEIVERS

I/Q Model	ϵ	ϕ
IQ1	1.0 dB	4°
IQ2	1.0 dB	7°
IQ3	1.6 dB	4°
IQ4	1.6 dB	7°

The received signal, for a MC scheme after CP removal, in the presence of I/Q imbalance (at the transmitter only) is given by $\mathbf{Y} = \tilde{\mathbf{X}} \otimes \mathbf{h} + \mathbf{n}$, where $\tilde{\mathbf{X}} = \alpha \mathbf{X} + \beta \mathbf{X}^{\dagger}$. The vector samples at the output of the FFT block after equalization are given by $\hat{x}_m = \alpha x_m + \beta \mathcal{F}_m\left(\mathbf{X}^{\dagger}\right) + \frac{\mathcal{F}_m(\mathbf{n})}{\mathcal{F}_m(\mathbf{h})}$. Therefore we get $\kappa_m = \alpha$ and $\zeta_m = \beta \mathcal{F}_m\left(\mathbf{X}^{\dagger}\right)$, where $\mathbf{X} = \left(\mathcal{F}_0^{-1}(\mathbf{x}), \ldots, \mathcal{F}_{N-1}^{-1}(\mathbf{x})\right)$. The baseband modulated symbol x_m in case of a MC scheme therefore experiences a common multiplication term (CMT) i.e. α which is the same for all symbols. This will have the effect of constellation rotation and contraction (since α is complex). An additional additive interference ζ_m will result in constellation clustering.

The received signal after CP removal and channel equalization for a SC scheme is given as $\hat{x}_m = \alpha x_m + \beta x_m^{\dagger} + \mathcal{F}_m^{-1}(\mathbf{N})$. The multiplicative and additive terms are thus given as $\kappa_m = \alpha$ and $\zeta_m = \beta x_m^{\dagger}$. Similar to the MC case the baseband modulated symbol in SC will also undergo constellation rotation, contraction and clustering. It is interesting to note here that unlike the MC scheme the additive interference of any symbol is dependent only on that symbol and β, whereas for MC scheme it depends on the β and the FFT of the modulated symbols, i.e., the interference is dependent on all the modulated symbols.

The I/Q imbalance results in a common multiplicative term (CMT) κ_m and an additive non zero term ζ_m for both MC and SC case. While both schemes suffer from the same CMT $\kappa_m = \alpha$, the additive term is different. Since $\mathbf{X}$ has a higher dynamic range than $\mathbf{x}$, the ζ_m term is enhanced in case of MC and therefore results in a relatively worse performance for the MC scheme as compared to the SC scheme. The SNR degradation as a function of the BER for SC and MC schemes using QPSK and 8PSK constellation for different I/Q parameters is shown in Figure 6. SC-QPSK outperforms MC-QPSK by about 0.7 dB at a BER of 10^{-4}, when $\epsilon = 1.0$ dB and $\phi = 4°$. For 8PSK constellations both SC and MC scheme exhibit very poor performance in the presence of I/Q imbalance and therefore must be used with some compensation algorithm to achieve satisfactory performance. However, the I/Q imbalance can easily be calibrated out.

C. Amplifier Nonlinearity: Model and Consequences

The input amplitude to output amplitude (AM/AM) and input amplitude to the output phase (AM/PM) relation for a nonlinear amplifier, when supplied with a complex input signal $a = |a| e^{j\phi_a}$, are denoted by $f(a)$ and $g(a)$ respectively. The amplifier output is given by $a_{out}(a) = af(a)e^{jg(a)}$. The input/output amplitude and phase relations for a typical power amplifier according to Saleh's model [12] are given as $f(a) = \frac{\alpha_f}{1+\beta_f |a|^2}$ and $g(a) = \frac{\alpha_g |a|^2}{1+\beta_g |a|^2}$, respectively. The parameters $\alpha_f, \beta_f, \alpha_g$ and β_g are device specific can be found by performing a minimum mean square curve fitting procedure [12]. The IBO of an amplifier is given as IBO $= \frac{a_{max}^2}{< P_{in} >}$, where $< P_{in} >$ denotes the average input power. The values for the amplifier model parameters used here are $\alpha_f = 1, \beta_f = 0.25, \alpha_g = \pi/50$ and $\beta_g = 0.25$ [13]. The normalized input/output relations for the given power amplifier parameters are shown in Figure 4, and are seen to be in good agreement with proposed 60 GHz HPA/LNA amplifier designs [5].

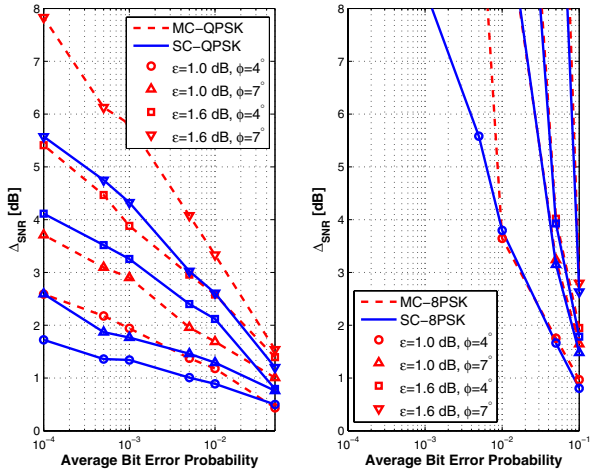

Fig. 6. SNR degradation as a function of BER for various I/Q imbalance parameters

The received MC signal, after CP removal and a nonlinear HPA is given by $\mathbf{Y} = \tilde{\mathbf{X}} \otimes \mathbf{h} + \mathbf{n}$, where the $\tilde{\mathbf{X}}$ is the OFDM symbol passed through a nonlinear amplifier, whose samples are given as $\tilde{X}_l = X_l f(X_l) e^{jg(X_l)}$. The vector samples at the output of the FFT block after equalization are given as $\hat{x}_m = \mathcal{F}_m\left(\tilde{\mathbf{X}}\right) + \frac{\mathcal{F}_m(\mathbf{n})}{\mathcal{F}_m(\mathbf{h})}$, where $\mathcal{F}_m\left(\tilde{\mathbf{X}}\right) = \left(\sum_{k=0}^{N-1} f(X_k) e^{jg(X_k)}\right) x_m + \sum_{n=0, n\neq m}^{N-1} x_n \sum_{k=0}^{N-1} f(X_k) e^{jg(X_k)} e^{j2\pi(n-m)k/N}$. This gives us $\kappa_m = \sum_{k=0}^{N-1} f(X_k) e^{jg(X_k)}$ and $\zeta_m = \sum_{n=0, n\neq m}^{N-1} x_n \sum_{k=0}^{N-1} f(X_k) e^{jg(X_k)} e^{j2\pi(n-m)k/N}$. The baseband modulated symbol therefore experiences a CMT i.e. κ_m and an additive interference ζ_m. The additive interference is seen to be dependent on the number of sub-carriers N, the amplifier nonlinearity transfer characteristics and the symbol mapping.

The received SC signal after CP removal and channel equalization is given as $\hat{x}_m = x_m f(x_m) e^{jg(x_m)} + \mathcal{F}_m^{-1}(\mathbf{N})$. The multiplicative and additive terms are $\kappa_m = f(x_m) e^{jg(x_m)}$ and $\zeta_m = 0$. In the SC scheme there is no additive interference experienced by the baseband symbol but only multiplicative noise κ_m which is independent of the block length N. The

multiplicative term is dependent only on the modulated symbol x_m and amplifier transfer characteristics.

The received MC signal is affected by CMT and additive interference. This results in clustering of the signal constellation points in addition to constellation contraction and rotation, whereas in SC, the only consequence is constellation rotation and contraction. The simulation results for SC and MC based system using QPSK and 8PSK constellations and employing nonlinear HPA are illustrated in Figure 7. Due to absence of ICI, the SC scheme clearly outperforms the MC scheme in terms of SNR degradation. For instance the SC-QPSK scheme outperforms the MC-QPSK by about 2.25 dB when the IBO is chosen to be 7 dB at a BER of 10^{-4}.

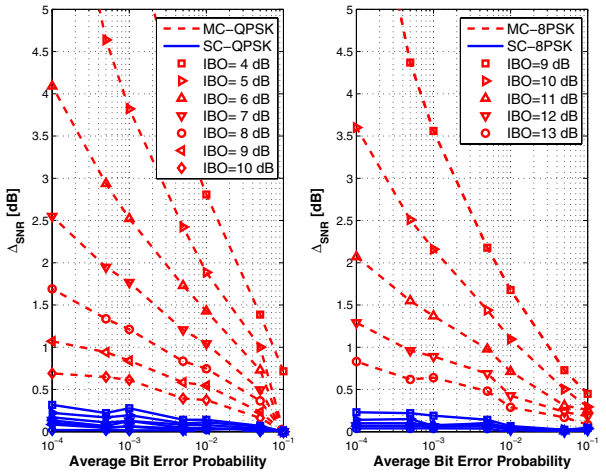

Fig. 7. SNR degradation as a function of BER for various IBO values of HPA

IV. Summary

The Δ_{SNR} in dB for the SC and MC schemes and a given set of RF system parameters, using QPSK and 8PSK constellations at a BER of 10^{-4} is summarized in Table III. The IBO values are specified in dB, phase noise is specified as the total integrated phase noise K in dBC and I/Q imbalance as amplitude imbalance ϵ in dB and phase imbalance ϕ in degrees. It can be seen that an un-coded SC system, while having the same implementation complexity, suffers a lower SNR degradation for all impairments except phase noise. However, from Figure 2 we see that SC scheme performs about 1 dB better than the MC scheme and the difference in performance for low phase noise variances i.e. PN3 between the SC and MC scheme is 0.1 dB and 0.9 dB at a BER of 10^{-4}. The SC scheme is therefore better for low phase noise variances while for high phase noise variances MC exhibits a lower degradation in SNR.

TABLE III

Δ_{SNR} FOR MC AND SC SCHEMES AT A BER OF 10^{-4}

Mod.	Transc.	PN	I/Q	HPA
QPSK	MC	0.9	2.6	4.1
$(K=-20, \epsilon=1, \phi=4, \text{IBO}=6)$	SC	1.1	1.8	0.3
8PSK	MC	0.9	-	3.6
$(K=-24, \epsilon=1, \phi=4, \text{IBO}=10)$	SC	1.8	-	0.2

V. Conclusions

In this paper, a comparison of SC and MC transmission schemes for 60 GHz systems, in the presence of RF circuit imperfections, was presented. PN, I/Q imbalance and HPA models, that are in accordance with 60 GHz transceiver circuits, were used. For both schemes the SNR degradation in terms of operating parameters such as the total integrated PN PSD and input back-off requirements for HPA was determined. It was shown that for high phase noise variances, the MC scheme suffers from a considerably lower SNR degradation, while SC can operate with a considerably lower HPA IBO. It was also shown that for multi-level constellations such as 8PSK the I/Q imbalance must be calibrated out for both SC and MC schemes.

VI. Acknowledgments

This work was supported by IOP GenCom under SiGi Spot project IGC.0503.

References

[1] D. Falconer, S. L. Ariyavisitakul, A. Benyamin-Seeyar, and B. Eidson, "Frequency domain equalization for single-carrier broadband wireless systems," *IEEE Communications Magazine*, vol. 40, no. 4, pp. 58–66, April 2002.

[2] Z. Wang, X. Ma, and G. B. Giannakis, "OFDM or single-carrier block transmissions?" *IEEE Transactions on Communications*, vol. 52, no. 3, pp. 380–394, March 2004.

[3] A. Seyedi and D. Birru, "On the design of a multi-gigabit short-range communication system in the 60 GHz band," in *Proc. IEEE Consumer Communications and Networking Conference*, January 2007.

[4] J. Tubbax, B. Come, L. V. Perre, L. Deneire, S. Donnay, and M. Engels, "OFDM versus single carrier with cyclic prefix: a system-based comparison," in *Proc. IEEE Vehicular Technology Conference*, October 2001, pp. 1115–1119.

[5] M. Kärkkäinen, M. Varonen, P. Kangaslahti, and K. Halonen, "Integrated amplifier circuits for 60 GHz broadband telecommunication," *Analog integrated circuits and signal processing*, vol. 42, pp. 37–46, Jun. 2005.

[6] C. Cao and K. K. O, "Millimeter-wave voltage-controlled oscillators on 0.13-um CMOS technology," *IEEE Journal of Solid State Circuits*, vol. 41, no. 6, pp. 1297–1304, June 2006.

[7] U. H. Rizvi, G. J. M. Janssen, and J. H. Weber, "Impact of RF circuit imperfections on multi-carrier and single-carrier based transmissions at 60 GHz," in *Proc. IEEE Radio and Wireless Symposium (accepted)*, January 2008.

[8] W. Lee, K. Kim, J. Kim, and Y. Kim. (2006, January) Multipath channel modeling 60 GHz frequency band. 15-06-0038-01-003c-multipath-channel-modeling-60ghz-frequency-band.ppt. [Online]. Available: ftp://ieee:wireless@ftp.802wirelessworld.com/15/06/

[9] A. Bourdoux and et. al., "Air interface and physical layer techniques for 60 GHz WPANs," in *Proc. IEEE Symposium on Communications and Vehicular Technology*, November 2006, pp. 1–6.

[10] M. Valkama, M. Renfors, and V. Koivunen, "Compensation of frequency-selective I/Q imbalances in wideband receivers: Models and algorithms," in *Proc. IEEE Workshop on Signal Processing Advances in Wireless Communications*, December 2001, pp. 42–45.

[11] B. Razavi, "A mm-wave CMOS heterodyne receiver with on-chip LO and driver," in *Proc. IEEE ISSCC Digest Technical Papers*, February 2007.

[12] A. A. M. Saleh, "Frequency-independent and frequency-dependent nonliner models of TWT amplifiers," *IEEE Transactions on Communications*, vol. COM-29, no. 11, pp. 1715–1720, November 1981.

[13] E. Costa and S. Pupolin, "M-QAM OFDM system performance in the presence of a nonlinear amplifier and phase noise," *IEEE Transactions on Communications*, vol. 48, no. 1, pp. 37–44, January 2000.